



Research article

Differential expression of α -L-arabinofuranosidase and α -L-arabinofuranosidase/ β -D-xylosidase genes during peach growth and ripening

M. Carolina Di Santo^a, Eduardo A. Pagano^a, Gabriel O. Sozzi^{a,b,*}

^aFacultad de Agronomía, Universidad de Buenos Aires, Avda. San Martín 4453, C1417DSE Buenos Aires, Argentina

^bConsejo Nacional de Investigaciones Científicas y Técnicas, Buenos Aires, Argentina

ARTICLE INFO

Article history:

Received 28 July 2008

Accepted 17 February 2009

Available online 28 February 2009

Keywords:

α -L-arabinofuranosidase

β -D-xylosidase

Peach

Prunus persica

Ripening

Softening

Ethylene

ABSTRACT

Arabinose is the major neutral sugar in peach (*Prunus persica* (L.) Batsch) cell walls and substantial changes in arabinose content take place not only during peach melting, when a rapid-softening-related depolymerizing activity may be expected, but also at the onset of peach ripening. A full-length cDNA clone sequence referred to as *PpARF1* (GenBank accession no. DQ486870) was obtained and determined by bioinformatics' analysis to be a peach α -L-arabinofuranosidase homologue. The deduced *PpARF1* translation product is 677 amino acids in length while the mature protein has a predicted molecular mass of 71.6 kD and a theoretical pI of 4.94. Semi-quantitative RT-PCR reactions were conducted to evaluate the expression of both *PpARF1* and *PpARF/XYL* (GenBank accession no. AB264280), the latter encoding a putative bifunctional protein displaying both α -L-arabinofuranosidase and β -D-xylosidase activities. In peach fruit, the *PpARF1* gene expression was detected at every developmental stage with a maximum during S2 (lag phase of development) and a subsequent decrease towards S4 (maximal fruit size). In contrast, *PpARF/XYL* transcript levels were relatively high at the end of S1 (fruit set) and at S3-E (beginning of the cell expansion). Substantial increases in *PpARF1* mRNA levels were found at the beginning and end of the climacteric rise and also in melting fruit. In contrast, *PpARF/XYL* transcripts reached a maximum when fruit firmness was 22–26 N, with a slight decline during the melting stage. *PpARF/XYL* and *PpARF1* were expressed differently in three fruit tissue types as well as in other plant tissues. Ethylene is regarded as the main regulator of peach ripening and the accumulation of *PpARF/XYL* and *PpARF1* transcripts is coincident with the autocatalytic ethylene production during ripening. On the hand, other factors may also play a role in *PpARF1* and *PpARF/XYL* expression, since transcripts accumulate at different developmental times and organs even when ethylene biosynthesis is barely detectable.

© 2009 Elsevier Masson SAS. All rights reserved.

1. Introduction

Because of its fruit, the peach tree (*Prunus persica* (L.) Batsch) is the most horticulturally valuable species in the subfamily *Prunoideae*. Genetic improvement for *Prunus* includes the achievement of high-quality fruit with long storage life [34]. Peach eating quality results from a unique combination of organoleptic characteristics [9] but firmness, usually measured with a penetrometer fitted with a 7.9-mm tip, is the best indicator of peach ripeness and a good predictor of its potential shelf life. Firmness is not regarded as more important to peach quality than flavor or aroma characters but factors that control firmness changes have probably been studied

more extensively. This is because the premature peach softening virtually ensures that it will deteriorate rapidly during storage, increasing its susceptibility to mechanical injury or pathogens.

Fruit softening is a complex process resulting from a plethora of changes at a morphological and cellular level [17]. Many of them are brought about by seemingly unrelated biochemical pathways. Because turgor pressure has a major influence on fruit texture in general [42] and on peach/nectarine texture in particular [18], water loss results not only in the loss of weight and appearance but also in a decrease in textural quality and in changes in fruit firmness. The plasma membrane is also expected to play a significant role both in the transport of cell-wall enzymes and materials and in the regulation of turgor pressure [17], aquaporin expression during ripening being an example of presumptive contribution to fruit turgor maintenance [24]. Nevertheless, the loss of firmness is mainly attributed to cell-wall degradation as a result of solubilization and/or depolymerization of cell-wall constituents [4].

* Corresponding author. Facultad de Agronomía, Universidad de Buenos Aires, Avda. San Martín 4453, C1417DSE Buenos Aires, Argentina. Tel.: +54 11 4524 8055; fax: +54 11 4514 8737.

E-mail address: gsozzi@agro.uba.ar (G.O. Sozzi).

Detailed studies of cell-wall polysaccharide metabolism in the so-called “model species” (mainly tomato and strawberry) have furthered much of the current knowledge about fruit softening but whether these models are applicable to other species is still debatable. In fact, the hypothesis of a highly conserved cell-wall metabolism is difficult to assemble with the significant variability between species/tissues in terms of cell-wall polysaccharide features and changes, and their regulation. The pectic and hemicellulosic polysaccharides of primary cell walls show a myriad of genotype-dependent conversions during fruit growth and ripening [4,6,42]. In peach, different cell wall-related enzymes/proteins and/or their putative coding genes have been studied, including exo and endopolygalacturonase (EC 3.2.1.67 and EC 3.2.1.15, respectively [12,26]), expansins [19], pectate lyases (EC 4.2.2.2 [20]), pectin-methylsterases (EC 3.1.1.11 [14]), endo-1,4- β -D-glucanases (EC 3.2.1.4 [3,20]), endo-1,4- β -mannanase (EC 3.2.1.78 [5]), α - and β -D-galactosidases (EC 3.2.1.22 and EC 3.2.1.23, respectively [21,22]) and α -L-arabinofuranosidase (α -L-arabinofuranoside arabinofuranohydrolase; EC 3.2.1.55 [4,20]). The study of peach glycosidases is, at least in part, a consequence from physiological and biochemical results showing that some glycosyl residues, mainly arabinose and galactose, display very dynamic roles during fruit development. In other fruit species such as tomato, pepper and muskmelon, galactose is considered the primary non-cellulosic neutral monosaccharide lost during development [4,16,27]. In contrast, arabinose is the major neutral sugar in the cell walls of peaches and nectarines although galactose is also present at relatively high levels [5,11,16]. Substantial changes in arabinose content take place not only during peach melting, when a rapid-softening-related depolymerizing activity may be expected, but also at the onset of peach ripening, simultaneous to the presence of α -L-arabinofuranosidase activity [5]. Nevertheless, α -L-arabinofuranosidase activity has also been detected at early stages of fruit development, when no apparent softening occurs [5] and may be related, at least in part, to a process of cell-wall reorganization rather than disorganization.

Recently, Hayama et al. [20] reported on a *PpARF/XYL* gene (GenBank accession no. AB264280) with very high sequence similarity to a putative peach β -D-xylosidase (EC 3.2.1.37) gene (*PpAz152* [28]; GenBank accession no. AF362990) and to the Japanese pear *PpARF2* (GenBank accession no. AB195230 [36]). The last one encodes a bifunctional protein displaying both α -L-arabinofuranosidase and β -D-xylosidase activities *in vitro* but only capable of catalyzing arabinose release from native cell-wall polysaccharides prepared from Japanese pear. *PpARF/XYL* mRNA did not accumulate in stony hard-flesh peaches but its levels increased after a continuous ethylene treatment. Also, *PpARF/XYL* transcript levels were barely noticeable during the first stages of melting-flesh peach softening but increased during ripening. Based on those results, *PpARF/XYL* was proposed to be a “softening-related gene” and the accumulation of its transcripts “completely ethylene dependent” [20]. The objective of this work was to report on the cloning and characterization of a new peach *PpARF* gene encoding a putative cell wall-related α -L-arabinofuranosidase and to compare its expression with that of *PpARF/XYL* in growing and ripening peaches, as well as in other plant organs.

2. Materials and methods

2.1. Plant material, and ethylene and firmness assessment

‘Springcrest’ peach samples were randomly picked from the orchard of the Facultad de Agronomía, Universidad de Buenos Aires (34° 37' 46" S; 58° 27' 46" W). Trees (‘Springcrest’/‘Nemaguard’) were planted and trained to a tatura-type trellis system and received standard cultural practices including: pruning, fruit

thinning, fertilization, irrigation and pest control. Peach seedling roots, intact mature leaves and open flowers were collected and flowers were dissected in sepals, petals, stamens (filaments plus anthers), and non-pollinated ovaries. Samples were immediately frozen in liquid nitrogen and stored at -80°C for later RNA analysis.

Fruit developmental stages (S1, S2, S3, and S4) were defined by using the first derivative of the growth cumulative curve, as previously described [7]. During growth, peaches were harvested and assigned to different physiological stages, and their age (days after full bloom, DAFB), size and ethylene production were registered (Fig. 1), as follows: S1 (34 DAFB; fruit set, end of the initial phase of exponential growth), S2 (39 DAFB; lag phase), early (S3-E) and late (S3-L) S3 (48 DAFB and 67 DAFB, respectively; cell expansion), and S4 (74 DAFB; immature full size fruit, pre-ripe or pre-climacteric). During ripening and softening, fruits were collected at each of five developmental stages as follows: R1 (onset), R2 (early-ripe), R3 (mid-ripe), R4 (fully ripe), R5 (overripe), on the basis of flesh firmness and ethylene production (Fig. 1). Three mm-thick mesocarp pieces, obtained from the equatorial region of each fruit at a site equidistant from the epicarp and the endocarp were sampled and immediately frozen in liquid nitrogen and stored at -80°C for later RNA analysis. Other samples from the same peaches were obtained and immediately processed for α -L-arabinofuranosidase extraction and activity assay as described below.

Additional tissues were collected from peach fruit. To compare transcript accumulation and α -L-arabinofuranosidase activity in different fruit tissues, peaches in stages S3-E, R1, R2 and R5 were selected and three fruit macrodomains were excised: the epicarp (including the outer epidermis and about 10 layers of hypodermal cells), the outer mesocarp (a 3 mm-thick region of mesocarp directly inward from the exocarp), and the inner mesocarp (a 3 mm-thick region of the inner mesocarp directly in contact with the hard endocarp). Several S3-E samples from each tissue were

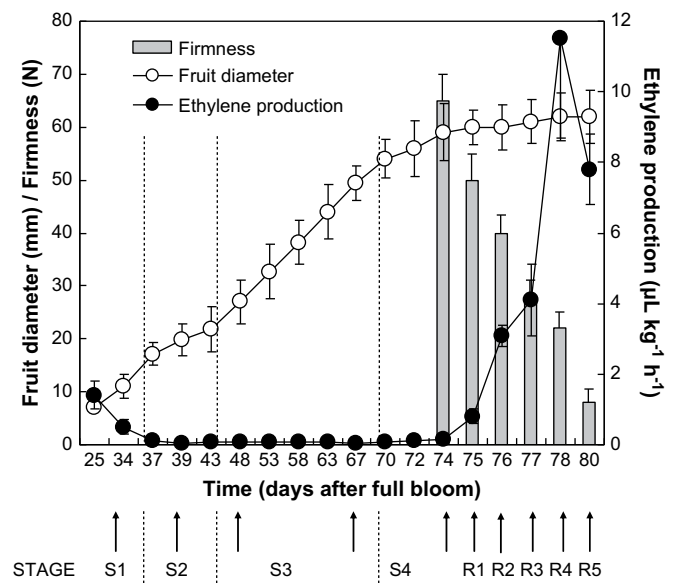


Fig. 1. Fruit diameter, ethylene production and firmness of ‘Springcrest’ peach fruit during development and ripening. Values represent the means \pm SD of 15 (ethylene and firmness) or 50 (diameter) replicates. Where bars are not shown, the SD does not exceed the size of the symbol. Stage transitions were determined according to Chalmers and van den Ende [7]. Stages were designed as follows: S1 (initial phase of exponential growth), S2 (lag phase), S3 (cell expansion phase), and S4 (immature full size fruit, pre-ripe or pre-climacteric). Ripening stages were designed as follows: R1 (onset, climacteric ethylene production beginning), R2 (early-ripe), R3 (mid-ripe), R4 (fully ripe, peak ethylene production), R5 (overripe). Arrows indicate the sampling dates for RNA analysis and/or α -L-arabinofuranosidase extraction and activity assay.

excised into liquid nitrogen and stored at -80°C for later RNA extraction but α -L-arabinofuranosidase extraction from S3-E, R1, R2 and R5 peaches and activity assay were performed immediately after excision, as described below.

Ethylene production was assessed by placing each peach in a 1.5-L glass container which was in turn tightly sealed with a lid with a silicon septum. One milliliter of the head-space gas was extracted after 1 h and ethylene was quantified on a Hewlett Packard 5890 Series II gas chromatograph (Agilent Technologies, Inc., Santa Clara, CA, USA) fitted with a FID and a stainless steel Porapak N column, as described elsewhere [40]. Fruit firmness was determined by measuring the force required to penetrate each fruit, with the skin removed, to a depth of 1 cm, using an Instron Universal Testing Machine (Model 3342, Canton, MA, USA). Each fruit was placed on a stationary steel plate. Two spots located on opposite sides of the fruit were punctured to a depth of 10 mm with a 7.9-mm diameter probe on a drill base with a cross-head setting of 50 mm min^{-1} , as previously described [33].

2.2. Isolation of cDNA clones

To clone an α -L-arabinofuranosidase homologue from *P. persica*, a set of degenerate and specific primers were designed against conserved amino acid residues of α -L-arabinofuranosidase from the following GenBank accession nos.: AY309436 (apple *MdAFase1*); AB073311 (Japanese pear *PpARF1*), and AB073310 (tomato *LeARF1*). These primers were used in standard PCR reactions containing cDNA from ripe peach mesocarp as template. Polyadenylated RNA was extracted from fruit mesocarp using the mRNA Isolation Kit (Roche Molecular Biochemicals, GmbH, Mannheim, Germany) and cDNA was made up with at least 10 ng of mRNA sample by means of Revert Aid™ M-Mul V Reverse transcriptase system (Fermentas International Inc., Burlington, Ontario, Canada). PCR conditions were as follows: 4 min at 94°C (first cycle); 45 s at 94°C , 45 s at 53 – 55°C , and 1 min at 72°C (35 cycles); and 7 min at 72°C (last cycle). Overlapping sequences were obtained using 4 different combinations of primers that covered the coding region of the gene except for the 3' end of the sequence. The primers for the 4 different PCR fragments were as follows: *fow Ara9d* 5' GTGGGTTGGAGTTGGA GTT 3', *rev AraR2* 5' TCCTCGATATTCATGCCCA 3' for 556 bp fragment; *fow AraL2* 5' TTCGAGGAGATTAATCACGC 3', *rev Ara4i* 5' CCAG GTCTCTCTCCAGGGTCCAA 3' for 701 bp fragment; *fow Ara4d* 5' AAGSGTGATATGGTTTGAYCAAGT 3', *rev Ara2i* 5' CCGTCGAGTTT GAAATCAT 3' for 586 bp fragment; *fow Ara8d* 5' GGAATTACCTTAA GTTCTA 3', *rev Ara3i* 5' TGAATGAACGCGGAGAGATT 3' for 770 bp fragment. PCR products were separated on 1.5% agarose gels, stained with SYBR Green (Invitrogen, Carlsbad, CA, USA) and visualized by the UVP Doc-It LS Image Acquisition Software. For sequencing, PCR products were cloned into the pGEM®-T Easy vector system (Promega Corp., Madison, WI, USA). The partial sequences were aligned and a 2254 bp contig sequence was obtained.

2.3. Rapid amplification of 3' cDNA ends

To obtain the 3' end of the sequence, cDNA was synthesized as described above using an oligo-dT adapter primer supplied in the Kit 3' RACE System for Rapid Amplification of cDNA Ends (Invitrogen, Carlsbad, CA, USA). Specific cDNA was then amplified by PCR using *Ara8d* (5' GGAAATACCTTAAGTTCTA 3') as gene-specific primer and an AUAP adapter primer that targets the poly(A) tail region.

2.4. Sequence analysis

Sequence analysis was performed on an ABI PRISM® 377 DNA Sequencer (Applied Biosystems, USA). The final sequence was

analyzed and homology searches were carried out using the NCBI BLAST algorithm (<http://www.ncbi.nlm.nih.gov/BLAST> [2]) on GenBank databases. Deduced amino acid sequence alignment and comparison were made by means of the ClustalW program (<http://www.ebi.ac.uk/clustalw> [37]). Open reading frame and protein prediction were made using NCBI ORF Finder (<http://www.ncbi.nlm.nih.gov/projects/gorf>). Protein domains were identified with the Simple Modular Architecture Research Tool (SMART; <http://smart.embl-heidelberg.de> [23]). Signal peptides and their cleavage sites were predicted using SignalP (<http://www.cbs.dtu.dk/services/SignalP> [25]) program. The subcellular location was predicted using the TargetP 1.1 Server (<http://www.cbs.dtu.dk/services/TargetP> [13]). The theoretical isoelectric point (pI) and mass values for mature peptides were calculated by means of the Compute pI/Mw tool (http://www.expasy.org/tools/pi_tool.html).

2.5. RT-PCR

Transcript accumulation of the cloned α -L-arabinofuranosidase homologue and *PpARF/XYL* gene was estimated through semi-quantitative RT-PCR reactions. Polyadenylated RNA was prepared from 250 mg of plant tissue as described below. mRNA concentration was quantified by measuring absorbance at 260 nm with an Agilent 8453 UV-Vis diode array spectrophotometer (Agilent Technologies, Inc., Santa Clara, CA, USA). The specific primers used were as follows: *fow AXF1* 5' GGTGCACAGATGTTTCATTGC 3', *rev AXR1* 5' TTTGCGAACGTGACATCAAT 3' for *PpARF/XYL* gene sequence (AB264280) that amplifies a 247 bp fragment; and *fow AraL2* 5' TTCGAGGAGATTAATCACGC 3', *rev AraR2* 5' TCCTCGATATTCATGCCCA 3' for *PpARF1* gene sequence (DQ486870) that amplifies a 283 bp fragment. PCR conditions were as follows: 4 min at 94°C (first cycle); 45 s at 94°C , 45 s at 54°C , and 1 min at 72°C (30 cycles for *PpARF/XYL* gene and 35 cycles for *PpARF1*); and 7 min at 72°C (last cycle). Actin was selected as a housekeeping gene, as it was found to be expressed at constant levels throughout fruit development and ripening, as well as in all other peach tissues tested (seedling roots, flower organs and mature leaves). Actin mRNA levels were utilized as internal controls to normalize the amount of starting template. The designed primers were as follows: *fow ActF1* 5' TGGCCGTGATCTAACAGATG 3', *rev ActR1* 5' CTGAGGAGCTGCT CTTTGCT 3' that amplifies a 164 bp fragment. PCR conditions were as described below except for the annealing temperature (55°C) and the number of cycles (25). PCR conditions for each primer pair were optimized empirically to determine the linear range of amplification. A 100-bp DNA ladder (Invitrogen, Carlsbad, CA, USA) was used as standard molecular marker. Each gel is representative of several replications.

2.6. α -L-Arabinofuranosidase activity

α -L-Arabinofuranosidase extraction and activity assay were performed as previously described [32], with minor differences. Summarizing, three composite mesocarp samples per date were homogenized in a blender (45 s) and then an Omnimixer (45 s) with 2 vol of cold 100 mM sodium acetate buffer, pH 4.5, containing 0.7 M NaCl, 1% (w/v) sucrose and 1.5% (w/v) PVPP. The subsequent steps were performed at 4°C . The suspension was filtered through several layers of Miracloth (Calbiochem Corp., La Jolla, CA) and centrifuged at $13\,000 \times g$ for 30 min. Aliquots of centrifuged extract were assayed for total activity. Reaction mixtures contained 250 μl of 0.1 M citrate buffer, pH 4.5, 200 μl of 0.1% bovine serum albumin, 50 μl of enzyme solution and 200 μl of 13 mM *p*-nitrophenyl- α -L-arabinofuranoside (Sigma Chemical Co., St. Louis, MO) as substrate solution, with incubation at 37°C . The generation of free *p*-nitrophenol remained linear for at least 2 h. Activities reported are based

on rates determined after 1 h, with the reaction stopped by addition of 1 ml of 0.2 M sodium carbonate. Absorbance was measured at 400 nm and free *p*-nitrophenol was used as standard. One unit of α -L-arabinofuranosidase activity was defined as the amount of enzyme hydrolyzing 1 μ g h⁻¹ of *p*-nitrophenyl- α -L-arabinofuranoside. Data of enzyme activities were expressed both on a per-gram fresh-weight basis and on a fruit basis. Three replications per sampling stage/tissue were evaluated.

3. Results and discussion

3.1. Isolation of a *PpARF1* cDNA clone and bioinformatics' analysis

Overlapping sequences were obtained using 4 different combinations of primers that covered the coding region of the gene except for the 3' end of the sequence. When the partial sequences were aligned, a 2254 bp contig sequence was obtained. The cloned cDNA contained a presumptive coding sequence of 2034 nucleotides. The full-length cDNA clone sequence (GenBank accession no. DQ486870) was determined by NCBI BLASTN analysis to be an α -L-arabinofuranosidase homologue and is herein referred to as *PpARF1*. Bioinformatic analysis revealed that *PpARF1* has between 85 and 88% mRNA identity with homologues from *Malus × domestica* (AY309436.1), *Pyrus communis* (AB067643.1), *Pyrus pyrifolia* (AB073311.1) and *Fragaria × ananassa* (EF635629.1) with a coverage ranging from 85 to 92%. The e-value reported by the BLASTN program for the first 10 sequences producing significant alignments was 0.0.

The deduced *PpARF1* translation product is 677 amino acids long (nucleotides 81–2114). The SignalP program predicted the presence of a 25 amino acid-long signal peptide in the *PpARF1* protein. The signal sequence present in the N terminus of *PpARF1* protein would be cleaved between the Ala and Ile residues at positions 25 and 26, respectively, resulting in a mature protein of 71.6 kD with a theoretical *pI* of 4.94. Similar values (*M_w* of 71.3 kD, theoretical *pI* of 4.74) were predicted for *MdARF1* [15]. The relatively low *pI* may be important for the precise positioning of the *PpARF1* protein in the wall since it may ionically interact with positively charged cell-wall molecules such as extensins – basic glycoproteins with *pI* of ~10 due to their Lys content.

The SMART program identified an α -L-arabinofuranosidase C-terminus of almost 200 residues (starting at position 460 and ending at 651), that catalyses the hydrolysis of non-reducing terminal α -L-arabinofuranosidic linkages in L-arabinose-containing polysaccharides. It also identified a carbohydrate binding module (CBM_4_9), starting at position 70 and ending at 235, although experimental evidence is still pending as to whether this domain actually confers binding. The TargetP 1.1 program strongly predicted that the encoded *PpARF1* protein could be exported to the apoplast thus suggesting that this putative α -L-arabinofuranosidase may be involved in cell-wall arabinosyl modification. In fact, most α -L-arabinofuranosidase activity is detected in high-salt released fractions, after tissue successive washings of the cell-wall pellet with a low-ionic strength buffer or water to remove cytosolic proteins [1], suggesting that α -L-arabinofuranosidase activity is by far chiefly attributable to cell-wall proteins. Ten presumptive N-glycosylation sites were predicted, based on the presence of the consensus tripeptide Asn-X-Ser/Thr (where X is any amino acid except Pro). Nevertheless, only 6 Asn were predicted to be glycosylated and just one N-glycosylation site, located at position 168 of the mature peptide, was found to have a high specificity (Asn very likely to be glycosylated).

The deduced amino acid sequence of *PpARF1* protein from peach was aligned with other plant sequences and a phylogenetic tree was constructed (Fig. 2). Bioinformatics' analysis of deduced amino

acid sequence alignments and phylogenetic examination revealed that *PpARF1* protein may be classified to glycoside hydrolase (GH) family 51, displaying between 83 and 86% amino acid identity with α -L-arabinofuranosidase homologues from apple (GenBank accession no. AY309436), Japanese pear (GenBank accession no. AB073311) and European pear (GenBank accession no. AB067643). This strong similarity suggests that these sequences are probably orthologous and that the encoded glycoside hydrolases are likely to have similar biochemical substrate specificities. Members of the GH family 51 usually hydrolyze relatively small substrates, including short-chain arabino-oligosaccharides. GH enzyme family 51 ([8; URL: <http://afmb.cnrs-mrs.fr/CAZY/>]) comprises α -L-arabinofuranosidase (EC 3.2.1.55) and endo- β -glucanase (EC 3.2.1.4) activities. Currently, the CAZy registers 193 entries in GH family 51 (<http://www.cazy.org/fam/GH51.html>); but very few tree fruit enzymes are listed with proven or predicted α -L-arabinofuranosidase activity while additional branches correspond to enzymes from other *Eukariota* or bacteria.

3.2. α -L-Arabinofuranosidase activity during fruit growth and ripening

A wide series of peach fruit development was chosen, based on fruit diameter, ethylene production and firmness (Fig. 1). Peaches were harvested for measurement of these indices, processed for α -L-arabinofuranosidase extraction and activity assay or sampled and immediately frozen in liquid nitrogen and stored at –80 °C for later RNA analysis, with no intervening storage period in order to represent as strictly as possible the natural peach development.

S1 fruit displayed relatively high total α -L-arabinofuranosidase activity levels on a fresh-weight basis but the activity declined during S2 and S3 reaching the lowest value at S3-L (Fig. 3). However, total fruit activity was relatively low at S1 and increased steadily in the pulp during the lag phase and cell expansion phase, decreasing as the end of S3 stage was reached. Brummell et al. detected relatively low specific α -L-arabinofuranosidase activity in half size 'O'Henry' peach fruit with a very slight increase until maximal fruit size was reached [5]. These differences may be due to genetic variations between cultivars (i.e., early- vs. late-season peaches) and/or to changes in the protein content per unit fresh weight, which certainly occurs as cells expand and accumulate water and solutes in vacuoles. Peaches evidenced a sharp increase in activity by the early-ripe stage (Fig. 3) as previously described [5], and reached a maximum at the ripe stage. Total α -L-arabinofuranosidase activity pattern throughout peach ontogeny is relatively similar to that of Japanese pear [35,36] and tomato fruit [31,32] despite the different fruit growth patterns between these species (double-sigmoid in peach; exponential early, then close to linear in Japanese pear and tomato). For Japanese pear and tomato, different isoforms are present at various stages through fruit development but only one ethylene-up-regulated isoform was found to participate in ripening-related cell-wall arabinose metabolism [32,36].

3.3. Temporal expression pattern of *PpARF1* and *PpARF/XYL* in fruit tissue

The temporal expression pattern of both *PpARF1* and *PpARF/XYL* genes in fruit tissue was examined using polyadenylated RNA [poly (A⁺) RNA] extracted from mesocarp tissue. *PpARF1* mRNA accumulation was detected at every developmental stage, with a maximum at S2 and a subsequent decrease towards S4 (Fig. 4). Remarkably, *PpARF1* transcript accumulation did not show a positive relationship with growth rate since its levels were higher in S2

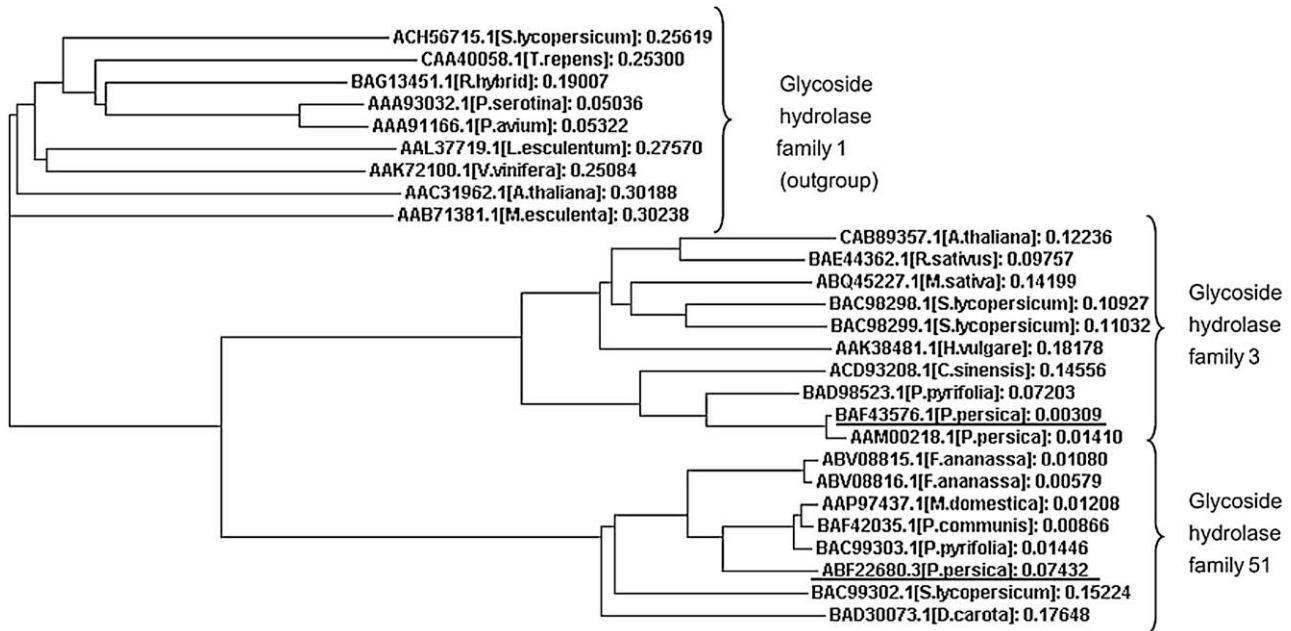


Fig. 2. Comparison of the deduced amino acid sequences of peach *PpARF1* and *PpARF/XYL* proteins with those of several plant α -L-arabinofuranosidases, α -L-arabinofuranosidase/ β -D-xylosidases and β -D-xylosidases. The phylogenetic tree was obtained from alignment of various published amino acid sequences classified to glycoside hydrolase families 1, 3 and 51, using the ClustalW program. The tree was rooted using the glycoside hydrolase family 1 as the outgroup. The NCBI protein accession number and the species are included in the phylogenetic tree, as follows: (A) Glycoside hydrolase family 1: beta-glucosidase O1 from *Solanum lycopersicum* (ACH56715.1); beta-glucosidase from *Trifolium repens* (CAA40058); beta-glucosidase from *Rosa hybrid* (BAG13451.1); prunasin hydrolase isoform PH I precursor from *Prunus serotina* (AAA93032); beta-glucosidase from *Prunus avium* (AAA91166.1); beta-mannosidase from *Lycopersicon esculentum* (AAL37719.1); beta-glucosidase from *Vitis vinifera* (AAK72100.1); beta-glucosidase from *Arabidopsis thaliana* (AAC31962.1); linamarase from *Manihot esculenta* (AAB71381.1); (B) Glycoside hydrolase family 3: beta-xylosidase-like protein from *Arabidopsis thaliana* (CAB89357.1); alpha-L-arabinofuranosidase from *Raphanus sativus* (BAE44362.1); beta-xylosidase/alpha-L-arabinosidase from *Medicago sativa* subsp. \times *varia* (ABQ45227.1); LEXYL1 (beta-D-xylosidase) from *Solanum lycopersicum* (BAC98298.1); LEXYL2 (beta-D-xylosidase) from *Solanum lycopersicum* (BAC98299.1); alpha-L-arabinofuranosidase/beta-D-xylosidase, isoenzyme ARA-I from *Hordeum vulgare* (AAK38481.1); beta-xylosidase from *Camellia sinensis* (ACD93208.1); alpha-L-arabinofuranosidase/beta-D-xylosidase from *Pyrus pyrifolia* (BAD98523.1); α -L-arabinofuranosidase/ β -D-xylosidase homologue from *Prunus persica* (BAF43576.1); beta-D-xylosidase from *Prunus persica* (AAM00218.1); (C) Glycoside hydrolase family 51: alpha-L-arabinofuranosidase from *Fragaria \times ananassa* (ABV08815.1); alpha-L-arabinofuranosidase from *Fragaria \times ananassa* (ABV08816.1); alpha-L-arabinofuranosidase from *Malus \times domestica* (AAP97437.1); alpha-arabinosidase1 from *Pyrus communis* (BAF42035.1); alpha-L-arabinofuranosidase from *Pyrus pyrifolia* (BAC99303.1); alpha-L-arabinofuranosidase from *Prunus persica* (ABF22680.3); alpha-L-arabinofuranosidase from *Solanum lycopersicum* (BAC99302.1); arabinofuranosidase from *Daucus carota* (BAD30073.1). Figures (numbers) after the species name indicate the relative phylogenetic distances between branches.

than in S3. Besides, *PpARF1* mRNA was also present at S3-L, when α -L-arabinofuranosidase activity was at its lowest level.

In contrast, the *PpARF/XYL* gene expression was relatively high only at specific developmental stages, namely S3-E and, to a lesser

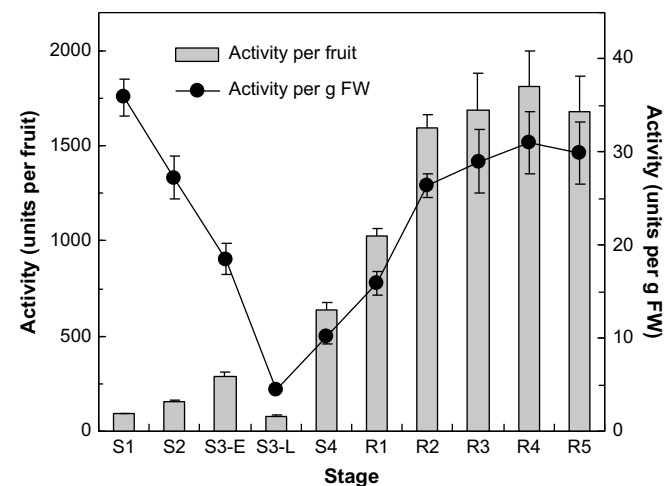


Fig. 3. Total α -L-arabinofuranosidase activity during growth and ripening. Activity is expressed both on a per-gram fresh-weight basis and on a fruit basis. One unit of activity was defined as the amount of enzyme hydrolyzing $1 \mu\text{g h}^{-1}$ of *p*-nitrophenyl- α -L-arabinofuranoside. All enzyme activities are expressed as the means \pm SD of three composite replicates.

extent, S1 (Fig. 4). These results suggest that transcription of *PpARF1* and *PpARF/XYL* is differentially regulated. *PpAz152*, with a very high sequence identity with *PpARF/XYL*, showed a similar expression pattern since transcripts were also found at early stages of fruit development [28]. Since the length of the 'Springcrest' peach fruit developmental stages in Buenos Aires is different from that in Padova [38], divergences in transcript levels during S3 between *PpAz152* [28] and *PpARF/XYL* (this work) may be attributed to differences in the exact moment in which the samples were

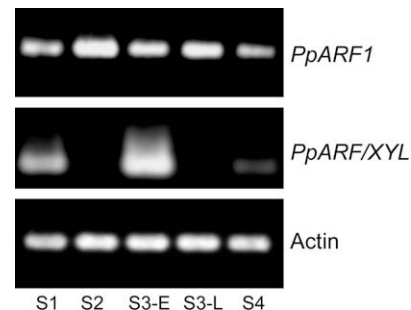


Fig. 4. *PpARF1* and *PpARF/XYL* transcript accumulation during peach fruit growth. Peaches were harvested and assigned to four different physiological stages, as follows: S1 (34 DAFB; fruit set, end of the initial phase of exponential growth), S2 (39 DAFB; lag phase), early (S3-E) and late (S3-L) S3 (48 DAFB and 67 DAFB, respectively; cell expansion phase), and S4 (74 DAFB; immature full size fruit, pre-ripe or pre-climacteric). Actin was used to evaluate equal loading.

obtained. In addition, α -L-arabinofuranosidase activity has proven not to be uniform in different regions of the mesocarp tissue (see also Section 3.4). Thus, variation in transcript levels can also derive from differences in the composition of the mesocarp samples.

The involvement of the product of the *PpAz152* gene in the response to pathogens has been suggested [28] based on its expression in young fruit and its wound-inducible characteristic. *PpARF1* and *PpARF/XYL* proteins, when present, might be implicated in defence responses against pathogens. Though there is no example for such a function in fruit tissues, some plant pathogenic fungi have arabinose-rich polysaccharides, and α -L-arabinofuranosidases may be required to lyse their mycelia.

Valero et al. [41] classified ripening peaches into three classes using previously established firmness criteria. The 35-N threshold is the minimum peach firmness to avoid bruising during standard postharvest handling when transferred to outlets. Peaches between 18 and 35 N are considered as “ready-to-buy” since they begin to yield to palm pressure and start to release their aroma. Finally, fruits below 18 N are regarded as “ready-to-eat”, although those ranging from 8 to 13 N are considered optimum for consumer acceptance [10]. These thresholds were selected as they indicate critical changes during postharvest ripening. *PpARF1*- and *PpARF/XYL*-related transcripts were present in every softening stage though at different accumulation levels (Fig. 5). *PpARF1* showed to be expressed throughout ripening, as is the case of its homologues in apple [15] and European pear [29]. Substantial increases in *PpARF1* mRNA levels were found in R2 (beginning of the climacteric rise), R4 (end of the climacteric rise) and R5 fruit (melting period of softening), while transcript levels were lower in R1 and R3. *PpARF/XYL* transcripts increased towards the R4 stage with an ensuing slight decline in the R5 stage. Using Northern blot analysis, Ruperti et al. found that *PpAz152* transcripts accumulate to significant levels during the late stages of fruit ripening [28] and Hayama et al. also found *PpARF/XYL* mRNA levels to have an increasing pattern during ripening [20]. In our study, maximum *PpARF/XYL* and *PpARF1* transcript levels are reached during R4 and R5 respectively, when higher total α -L-arabinofuranosidase activity was detected (Fig. 3). Also, this agrees with previous findings regarding massive losses of arabinose from loosely bound matrix glycans in R4 and R5, and an increase in the polymeric arabinose content of the CDTA-soluble fraction [5].

Fruit development and ripening involve a complex array of physiological and biochemical changes. *PpARF/XYL* was previously proposed to be a softening-related gene with an accumulation of transcripts coincident with autocatalytic ethylene production of the fruit [20]. In our work, ethylene production peaks at R4 with a slight decline in R5 (Fig. 1), while maximum *PpARF/XYL* and *PpARF1* transcript levels are reached during R4 and R5 respectively (Fig. 5). These results point towards the responsiveness of these genes to ethylene. However, to prove the direct ethylene involvement,

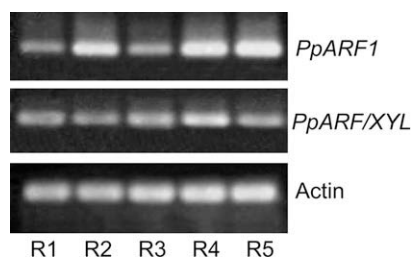


Fig. 5. *PpARF1* and *PpARF/XYL* transcript accumulation during peach fruit ripening. Peaches were collected at each of five ripening stages, as follows: R1 (onset, climacteric ethylene production beginning), R2 (early-ripe), R3 (mid-ripe), R4 (fully ripe, peak ethylene production), R5 (overripe). Actin was used to evaluate equal loading.

experiments with exogenous ethylene or an analogue, and an ethylene action inhibitor (e.g. 1-MCP, silver thiosulphate) are needed. On the other hand, our results show that *PpARF1* and *PpARF/XYL* transcript accumulation in fruit begins before the climacteric onset (Fig. 4). Moreover, *PpARF1* transcript accumulation peaks in S2 and *PpARF/XYL* mRNAs reach its peak in S3-E, even when ethylene levels are as low as $0.05 \mu\text{l kg}^{-1} \text{h}^{-1}$ thus suggesting that transcription of these genes may also be regulated by factors other than ethylene. Results herein presented do not question the responsiveness of *PpARF/XYL* to ethylene [20] but suggest that *PpARF/XYL* expression may also depend on other factors. Actually, Trainotti et al. strongly suggested a role of its own for auxin during peach ripening as well as an important cross-talk between auxin and ethylene [39]. This interplay between auxin and ethylene is supported by microarray experiments demonstrating significant transcription changes at the onset of ripening and an effect of 1-MCP on the expression of some auxin metabolism-related genes [43]. Although no experiments have been performed to examine the responsiveness of *PpARF/XYL* and *PpARF1* transcription to auxin, different α -L-arabinofuranosidases have been found to be modulated by synthetic auxins, both in tomato pericarp discs [32] and in apple callus [1].

3.4. Spatial expression pattern of *PpARF1* and *PpARF/XYL* in peach fruit

Total α -L-arabinofuranosidase activity was measured in three specific tissues during S3-E, R1, R2 and R5 (Fig. 6). Activity was higher in the inner pericarp and lower in the outer pericarp in all stages assayed except for R1. In S3-E, R2 and R5 peaches, the epicarp displayed levels of activity in-between those of the other two tissues.

RT-PCR analysis was performed to determine transcript accumulation in specific tissues within S3-E immature fruit (Fig. 7). Both *PpARF1* and *PpARF/XYL* transcripts were detected at a far more abundant level in the inner mesocarp. *PpARF/XYL* mRNA was also detected within the peel and the outer mesocarp, albeit at lower levels. In contrast, *PpARF1* transcript accumulation was hardly

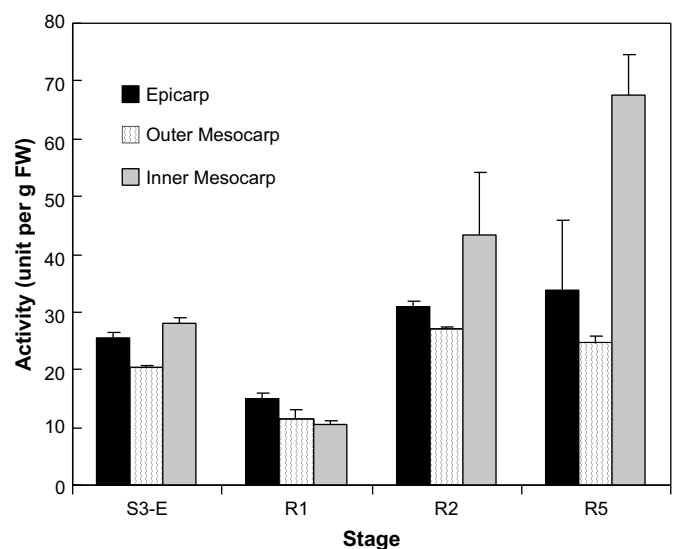


Fig. 6. Total α -L-arabinofuranosidase activity in three different fruit tissues (epicarp, outer mesocarp and inner mesocarp) during growth and ripening. Activity is expressed on a per-gram fresh-weight basis. One unit of activity was defined as the amount of enzyme hydrolyzing $1 \mu\text{g h}^{-1}$ of *p*-nitrophenyl- α -L-arabinofuranoside. All enzyme activities are expressed as the means \pm SD of three composite replicates.

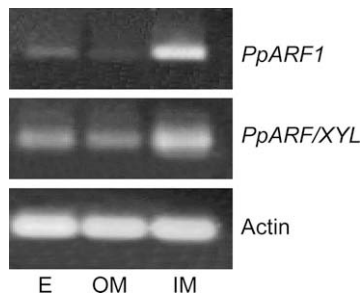


Fig. 7. *PpARF1* and *PpARF/XYL* transcript accumulation in three different S3-E fruit tissues. Tissues are as follows: epicarp (E), outer mesocarp (EM), inner mesocarp (IM). Actin was used to evaluate equal loading.

noticeable in the epicarp and in the outer mesocarp. Cell division continues for a longer time period in the epi- and hypodermis, due to the expansion of the fruit and its growth in circumference. This may partially explain the accumulation of higher levels of *PpARF/XYL* transcripts in the skin than in the outer mesocarp.

Because the pericarp of peaches contains at least three different tissue types and these show markedly different *PpARF1* and *PpARF/XYL* expression, diverse macrodomains in the fruit are feasible to display different cell-wall polysaccharide metabolism. Even if the peel is separated, the homogenization of the entire mesocarp will mask subtle changes associated with ripening/softening within specific tissue types. Although no spatial expression pattern was followed during ripening/softening in this study, it is possible that ripening peaches bear tissues at different maturity stages and with different *PpARF1* and *PpARF/XYL* expression patterns, since ripening usually starts on the inside of peach fruit and proceeds outwards. Peach exposure to ethylene or its analogues is a routine treatment in laboratory protocols [20] since ethylene readily diffuses within the fruit tissue. Nevertheless, it cannot be ruled out that ethylene-treated peaches might display a somewhat different pattern of expression, with higher *PpARF/XYL* transcript accumulation in the outer mesocarp in comparison to that in ripening untreated fruit.

3.5. Tissue specificity

RT-PCR analysis was also performed to find whether *PpARF1* and *PpARF/XYL* were expressed in non-fruit tissues. Both *PpARF1* and *PpARF/XYL* transcripts were present in every vegetative and reproductive tissue tested (Fig. 8). In vegetative organs, maximum *PpARF1* mRNA was found in sepals while maximum *PpARF/XYL* mRNA accumulation occurred in mature leaves and sepals. To a lesser extent, *PpARF1* and *PpARF/XYL* transcript accumulation was

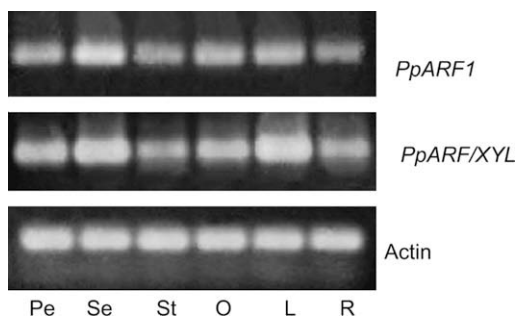


Fig. 8. *PpARF1* and *PpARF/XYL* transcript accumulation in peach flowers, intact expanded leaves (L) and seedling roots (R). Flower organs are as follows: petals (Pe), sepals (Se), stamens (St) and non-pollinated ovaries (Ov). Actin was used to evaluate equal loading.

found in other flower organs and in roots. mRNA corresponding to *PpAz152* (a gene with very high sequence similarity to *PpARF/XYL*) was found in RNA samples from flowers at all developmental stages and during leaf senescence [28]. The expression of these genes in non-fruit tissues does not exclude a softening-related role as happens with the gene encoding tomato β -galactosidase II [30].

4. Conclusion

In this work, a full-length cDNA clone sequence referred to as *PpARF1* was obtained and determined by bioinformatics' analysis to be a peach α -L-arabinofuranosidase homologue. In peach, the climacteric occurs after fruits have already started to soften. *PpARF1* and *PpARF/XYL* proteins, when present, might be involved both in the growth and softening processes, although cell-wall arabinose content does not change significantly during growth events, which suggests a reorganization of pectins and/or hemicelluloses within the cell wall rather than mobilization therefrom. The accumulation of *PpARF/XYL* and *PpARF1* transcripts is coincident with autocatalytic ethylene production during ripening and these genes could be considered softening-related. On the other hand, our results suggest that *PpARF1* and *PpARF/XYL* transcript accumulation begins before the climacteric onset. Moreover, both *PpARF1* and *PpARF/XYL* mRNAs accumulate at different developmental times and organs even when ethylene levels are low. Results presented herein do not question the responsiveness of *PpARF/XYL* to ethylene but suggest that transcription of these genes may also be regulated by factors other than ethylene (e.g. auxins).

Acknowledgements

G.O.S. thanks the Consejo Nacional de Investigaciones Científicas y Técnicas, the Universidad de Buenos Aires (UBACyT Program) and the Agencia Nacional de Promoción Científica y Tecnológica for financial support. M.C.D.S. is an addressee of a doctoral fellowship from the Consejo Nacional de Investigaciones Científicas y Técnicas, Argentina.

References

- [1] P. Alayón-Luaces, E.A. Pagano, L.A. Mroginski, G.O. Sozzi, Four glycoside hydrolases are differentially modulated by auxins, cytokinins, abscisic acid and gibberellic acid, in apple fruit callus cultures, *Plant Cell Tissue Org. Cult.* 95 (2008) 257–263.
- [2] S.F. Altschul, T.L. Madden, A.A. Schäffer, J. Zhang, Z. Zhang, W. Miller, D.J. Lipman, Gapped BLAST and PSI-BLAST: a new generation of protein database search programs, *Nucl. Acids Res.* 25 (1997) 3389–3402.
- [3] C. Bonghi, L. Ferrarese, B. Ruperti, P. Tonutti, A. Ramina, Endo- β -1,4-glucanases are involved in peach fruit growth and ripening, and regulated by ethylene, *Physiol. Plant.* 102 (1998) 346–352.
- [4] D.A. Brummell, Cell wall disassembly in ripening fruit, *Funct. Plant Biol.* 33 (2006) 103–119.
- [5] D.A. Brummell, V. Dal Cin, C.H. Crisosto, J.M. Labavitch, Cell wall metabolism during maturation, ripening and senescence of peach fruit, *J. Exp. Bot.* 55 (2004) 2029–2039.
- [6] D.A. Brummell, M.H. Harpster, Cell wall metabolism in fruit softening and quality and its manipulation in transgenic plants, *Plant Mol. Biol.* 47 (2001) 311–340.
- [7] D.J. Chalmers, B. van den Ende, A reappraisal of the growth and development of peach fruit, *Aust. J. Plant Physiol.* 2 (1975) 623–634.
- [8] P.M. Coutinho, B. Henrissat, Carbohydrate-active enzymes: an integrated database approach, in: H.J. Gilbert, G. Davies, B. Henrissat, B. Svensson (Eds.), *Recent Advances in Carbohydrate Bioengineering*, The Royal Society of Chemistry, Cambridge, UK, 1999, pp. 3–12.
- [9] C.H. Crisosto, G.M. Crisosto, G. Echeverría, J. Puy, Segregation of peach and nectarine (*Prunus persica* (L.) Batsch) cultivars according to their organoleptic characteristics, *Postharvest Biol. Technol.* 39 (2006) 10–18.
- [10] C.H. Crisosto, F.G. Mitchell, Postharvest handling systems: stone fruits, in: A.A. Kader (Ed.), *Postharvest Technology of Horticultural Crops*, third ed. University of California, Agriculture and Natural Resources, California, USA, 2002, pp. 345–352 Publication 3311.

- [11] D.M. Dawson, L.D. Melton, C.B. Watkins, Cell wall changes in nectarines (*Prunus persica*). Solubilization and depolymerization of pectic and neutral polymers during ripening and in mealy fruit, *Plant Physiol.* 100 (1992) 1203–1210 [correction in *Plant Physiology* 102 (1993) 1062–1063].
- [12] C.G. Downs, C.J. Brady, A. Gooley, Exopolysaccharuronase protein accumulates late in peach fruit ripening, *Physiol. Plant.* 85 (1992) 133–140.
- [13] O. Emanuelsson, H. Nielsen, S. Brunak, G. von Heijne, Predicting subcellular localization of proteins based on their N-terminal amino acid sequence, *J. Mol. Biol.* 300 (2000) 1005–1016.
- [14] H. Glover, C. Brady, Purification of three pectin esterases from ripe peach fruit, *Phytochemistry* 37 (1994) 949–955.
- [15] L.F. Goulao, D.J. Cosgrove, C.M. Oliveira, Cloning, characterisation and expression analyses of cDNA clones encoding cell wall-modifying enzymes isolated from ripe apples, *Postharvest Biol. Technol.* 48 (2008) 37–51.
- [16] K.C. Gross, C.E. Sams, Changes in cell wall neutral sugar composition during fruit ripening: a species survey, *Phytochemistry* 23 (1984) 2457–2461.
- [17] F.R. Harker, R.J. Redgwell, I.C. Hallett, S.H. Murray, G. Carter, Texture of fresh fruit, *Hortic. Rev.* 20 (1997) 121–224.
- [18] F.R. Harker, P.W. Sutherland, Physiological changes associated with fruit ripening and the development of mealy texture during storage of nectarines, *Postharvest Biol. Technol.* 2 (1993) 269–277.
- [19] H. Hayama, A. Ito, T. Moriguchi, Y. Kashimura, Identification of a new expansin gene closely associated with peach fruit softening, *Postharvest Biol. Technol.* 29 (2003) 1–10.
- [20] H. Hayama, T. Shimada, H. Fujii, A. Ito, Y. Kashimura, Ethylene regulation of softening and softening-related genes in peach, *J. Exp. Bot.* 57 (2006) 4071–4077.
- [21] E.M. Kupferman, W.H. Loescher, Glycosidase activities and development of peach fruit mesocarp tissues, *J. Am. Soc. Hort. Sci.* 105 (1980) 452–454.
- [22] D.H. Lee, S.-G. Kang, S.-G. Suh, J.K. Byun, Purification and characterization of a β -galactosidase from peach (*Prunus persica*), *Mol. Cells* 15 (2003) 68–74.
- [23] I. Letunic, R.C. Copley, B. Pils, S. Pinkert, J. Schultz, P. Bork, SMART 5: domains in the context of genomes and networks, *Nucl. Acids Res.* 34 (2006) D257–D260.
- [24] P. Mut, C. Bustamante, G. Martínez, K. Alleva, M. Sutka, M. Civallo, G. Amodeo, A fruit-specific plasma membrane aquaporin subtype PIP1;1 is regulated during strawberry (*Fragaria x ananassa*) fruit ripening, *Physiol. Plant.* 132 (2008) 538–551.
- [25] H. Nielsen, J. Engelbrecht, S. Brunak, G. von Heijne, Identification of prokaryotic and eukaryotic peptides and prediction of their cleavage sites, *Protein Eng.* 10 (1997) 1–6.
- [26] R. Pressey, J.K. Avants, Separation and characterization of endopolysaccharuronase and exopolysaccharuronase from peaches, *Plant Physiol.* 52 (1973) 252–256.
- [27] R.J. Redgwell, M. Fischer, E. Kendal, E.A. MacRae, Galactose loss and fruit ripening: high-molecular-weight arabinogalactans in the pectic polysaccharides of fruit cell walls, *Planta* 203 (1997) 174–181.
- [28] B. Ruperti, L. Cattivelli, S. Pagni, A. Ramina, Ethylene-responsive genes are differentially regulated during abscission, organ senescence and wounding in peach (*Prunus persica*), *J. Exp. Bot.* 53 (2002) 429–437.
- [29] D. Sekine, I. Munemura, M. Gao, W. Mitsuhashi, T. Toyomasu, H. Murayama, Cloning of cDNAs encoding cell-wall hydrolases from pear (*Pyrus communis*) fruit and their involvement in fruit softening and development of melting texture, *Physiol. Plant.* 126 (2006) 163–174.
- [30] D.L. Smith, D.A. Starrett, K.C. Gross, A gene coding for tomato fruit β -galactosidase II is expressed during fruit ripening. Cloning, characterization, and expression pattern, *Plant Physiol.* 117 (1998) 417–423.
- [31] G.O. Sozzi, A.A. Fraschina, A.A. Navarro, O. Cascone, L.C. Greve, J.M. Labavitch, α -L-Arabinofuranosidase activity during development and ripening of normal and ACC synthase antisense tomato fruit, *HortScience* 37 (2002) 564–566.
- [32] G.O. Sozzi, L.C. Greve, G.A. Prody, J.M. Labavitch, Gibberellic acid, synthetic auxins, and ethylene differentially modulate α -L-arabinofuranosidase activities in antisense 1-aminocyclopropane-1-carboxylic synthase tomato pericarp discs, *Plant Physiol.* 129 (2002) 1330–1340.
- [33] G.O. Sozzi, G.D. Trincherro, A.A. Fraschina, Delayed ripening of 'Bartlett' pears treated with nitric oxide, *J. Hortic. Sci. Biotechnol.* 78 (2003) 899–903.
- [34] C. Srinivasan, I.M.G. Padilla, R. Scorza, *Prunus* spp. Almond, apricot, cherry, nectarine, peach and plum, in: R.E. Litz (Ed.), *Biotechnology of Fruit and Nut Crops*, CABI Publishing, Wallingford, Oxfordshire, UK, 2005, pp. 512–542.
- [35] A. Tateishi, Y. Kanayama, S. Yamaki, α -L-Arabinofuranosidase from cell walls of Japanese pear fruits, *Phytochemistry* 42 (1996) 295–299.
- [36] A. Tateishi, H. Mori, J. Watari, K. Nagashima, S. Yamaki, H. Inoue, Isolation, characterization, and cloning of α -L-arabinofuranosidase expressed during fruit ripening of Japanese pear, *Plant Physiol.* 138 (2005) 1653–1664.
- [37] J.D. Thompson, D.J. Higgins, T.J. Gibson, CLUSTALW: improving the sensitivity of progressive multiple sequence alignment through sequence weighting, position-specific gap penalties and weight matrix choice, *Nucl. Acids Res.* 22 (1994) 4673–4680.
- [38] P. Tonutti, C. Bonghi, B. Ruperti, G.B. Torioli, A. Ramina, Ethylene evolution and 1-aminocyclopropane-1-carboxylate oxidase gene expression during early development and ripening of peach fruit, *J. Am. Soc. Hort. Sci.* 122 (1997) 642–647.
- [39] L. Trainotti, A. Tadiello, G. Casadoro, The involvement of auxin in the ripening of climacteric fruits comes of age: the hormone plays a role of its own and has an intense interplay with ethylene in ripening peaches, *J. Exp. Bot.* 58 (2007) 3299–3308.
- [40] G.D. Trincherro, G.O. Sozzi, A.M. Cerri, F. Vilella, A.A. Fraschina, Ripening-related changes in ethylene production, respiration rate and cell-wall enzyme activity in goldenberry (*Physalis peruviana* L.), a solanaceous species, *Postharvest Biol. Technol.* 16 (1999) 139–145.
- [41] C. Valero, C.H. Crisosto, D. Slaughter, Relationship between nondestructive firmness measurements and commercially important ripening fruit stages for peaches, nectarines and plums, *Postharvest Biol. Technol.* 44 (2007) 248–253.
- [42] A.R. Vicente, M. Saladié, J.K.C. Rose, J.M. Labavitch, The linkage between cell wall metabolism and fruit softening: looking to the future, *J. Sci. Food Agric.* 87 (2007) 1435–1448.
- [43] F. Ziliotto, M. Begheldo, A. Rasori, C. Bonghi, P. Tonutti, Transcriptome profiling of ripening nectarine (*Prunus persica* L. Batsch) fruit treated with 1-MCP, *J. Exp. Bot.* 59 (2008) 2781–2791.